ISSN 1069-3513, Izvestiya, Physics of the Solid Earth, 2025, Vol. 61, No. 3, pp. 318–333. © Pleiades Publishing, Ltd., 2025.

Paleomagnetism of Miocene Magmatic Formations in South Kamchatka

A. V. Latyshev[a, b, c] *, M. B. Anosova[b, c], E. A. Latanova[b, d], and O. V. Bergal-Kuvikas[c, e]

[a] *Moscow State University, Faculty of Geology, Moscow, 119991 Russia*

[b] *Schmidt Institute of Physics of the Earth, Russian Academy of Sciences, Moscow, 123242 Russia*

[c] *Institute of Volcanology and Seismology, Far Eastern Branch, Russian Academy of Sciences, Petropavlovsk-Kamchatsky, 683000 Russia*

[d] *National University of Science and Technology "MISiS," Moscow, 119049 Russia*

[e] *Vitus Bering Kamchatka State University Petropavlovsk-Kamchatsky, 684090 Russia*

**e-mail: anton.latyshev@gmail.com*

Received March 26, 2024; revised August 27, 2024; accepted August 28, 2024

Abstract—Reconstructing the tectonic evolution of Kamchatka is crucial for deciphering the mechanisms of fold belt formation and development of subduction systems. This requires reliable paleomagnetic information for the poorly studied segments of the Koryak–Kamchatka fold region such as southern Kamchatka. This paper presents the first paleomagnetic data on Miocene magmatic bodies of the Pribrezhny complex, which is widespread on the Pacific coast of southern Kamchatka. The paleomagnetic pole calculated for the Miocene of southern Kamchatka from 33 sites is statistically significantly different from all the published Cenozoic poles in the nearby regions. The new data indicate the formation of Miocene volcanics at a paleolatitude close to the present position (52.3°) and support the formation of the Miocene supra-subduction volcanic belt on the more ancient basement of the Olyutor–Kamchatka fold system rather than within a separate exotic block. It is shown that most of the sampled volcanics formed before the main phase of tectonic deformation, but at least part of the studied normal-polarity bodies contain postfolding magnetization and may represent products of younger episodes of magmatism.

Keywords: paleomagnetism, magnetic properties, Kamchatka, Miocene, supra-subduction volcanism, tectonics, Pribrezhny volcanic complex

DOI: 10.1134/S1069351325700351

1. INTRODUCTION

Kamchatka is a unique example of a modern active continental margin and an active volcanic region in the territory of Russia. This makes deciphering the tectonic evolution of Kamchatka crucial for understanding the mechanisms of fold formation and tectono-magmatic evolution of subduction systems. Despite this, many issues remain controversial even in the Cenozoic history of Kamchatka. In particular, all modern tectonic reconstructions of this segment of the northwestern Pacific are based on paleomagnetic data for northern Kamchatka alone (Kovalenko, 1992; 2003; Pecherskiy et al., 1997; Levashova et al., 1998; 2000; Bazhenov et al., 2001; Kovalenko and Chernov, 2003; Vaes et al., 2019). The structural affiliation of southern Kamchatka remains a subject of debate. Various tectonic schemes consider this region part of the Olyutor–Kamchatka fold system with an overlying Neogene volcanic belt (Zonenshain et al., 1990), a continuation of the Kuril Island arc that has existed since the Oligocene (Avdeiko et al., 2006; Khanchuk and Grebennikov, 2021), or an independent tectonic block (Bogdanov and Chekhovich, 2002).

Cenozoic magmatic complexes are widespread in southern Kamchatka, but their structural position and the geodynamic setting of their formation are still unclear. Initially, these magmatic formations were combined into the "Miocene andesite formation" of southern Kamchatka (Sheimovich and Patoka, 1989). The 1 : 200000 State Geological Map distinguishes the Zavoiko, Akhomten, and Asacha Miocene complexes in this region (Sheimovich et al., 2000). In the latest version of the 1 : 1000000 State Geological Map (Slyadnev et al., 2006), the volcanic formations of southern Kamchatka are combined into the Oligocene–Miocene Pribrezhny volcanic complex. In this paper, the latter is referred to as Pribrezhny complex.

The age of the Pribrezhny complex magmatics is primarily determined by the K-Ar dating estimates ranging between 20.5 and 9.6 Ma (Sheimovich et al., 2000), which corresponds to the early Miocene. Our recent isotopic dating estimates narrow this range

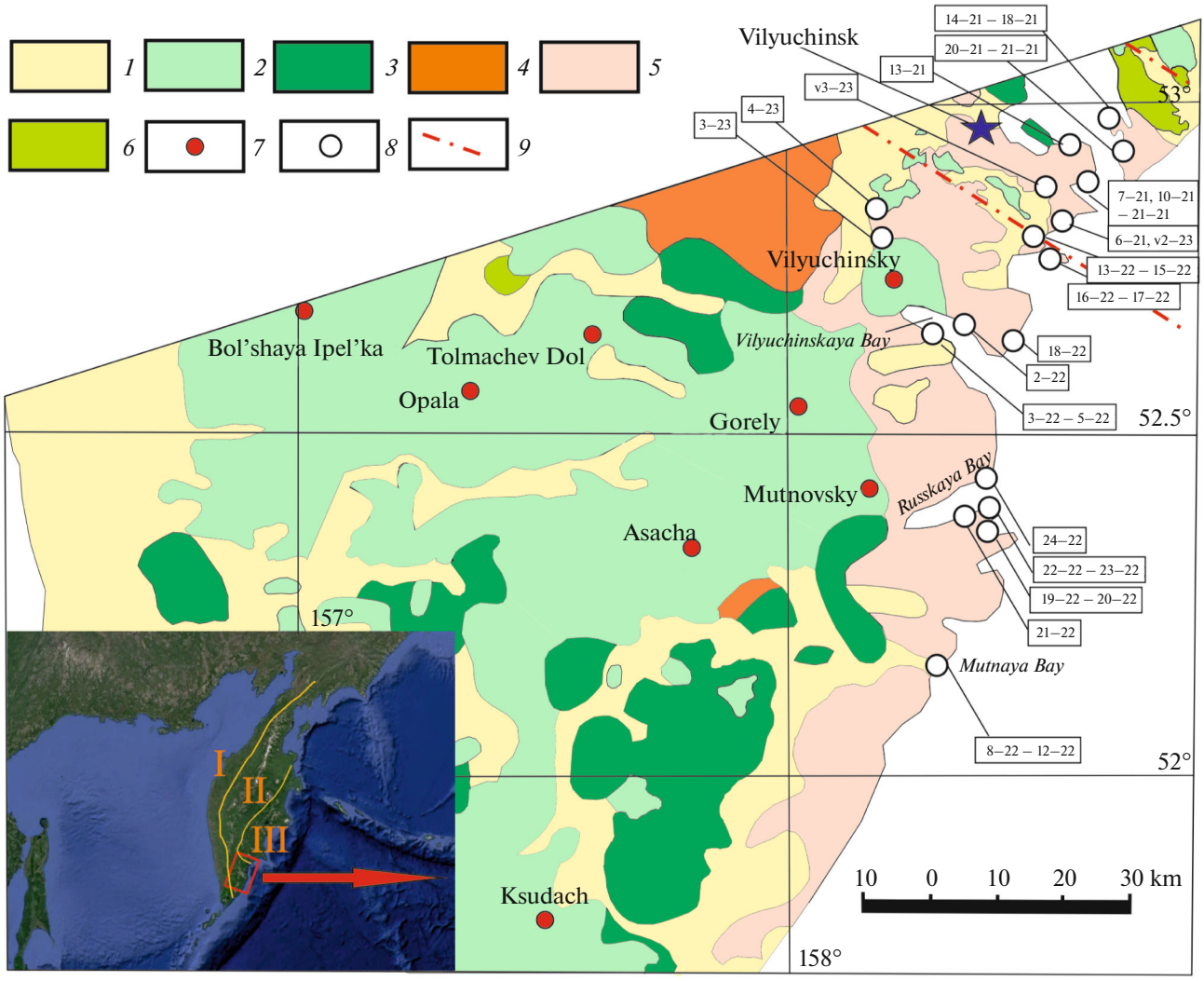

Fig. 1. Geological map of study region (based on (Sheimovich and Patoka, 1989), with modifications). *1*, Eocene–Quaternary terrigenous deposits; *2*, Pleistocene–Holocene volcanic formations; *3*, Pliocene volcanics of mainly basaltic and basaltic andesite composition; *4*, Pliocene–Pleistocene volcanics of mainly dacite–rhyolite composition; *5*, Miocene magmatic formations of the Pribrezhny complex; *6*, Cretaceous magmatic and metamorphic formations; *7*, large Quaternary volcanic centers; *8*, sampling points; *9*, boundaries of Malka–Petropavlovsk transverse fault zone. Inset shows boundaries of tectonic zones according to (Zonenshain et al., 1990; Nikishin et al., 2009), with changes: I, Koryak–West Kamchatka terrain belt; II, Olyutor–Mid-Kamchatka terrain belt; III, Kronotsky terrane.

somewhat (19.1–13.2 Ma (Bergal-Kuvikas et al., in press)) but confirm the early Miocene age of the main magmatic phase. Thus, the Pribrezhny complex volcanics are older than the final stage of folding deformation within Kamchatka associated with the accretion of the Kronotsky island arc terrain 10–5 Myr ago, which corresponds to the end of the Miocene (Levashova et al., 2000; Solov'ev et al., 2004; Lander and Shapiro, 2007). At the same time, the Pribrezhny complex extends northward to Petropavlovsk-Kamchatsky, where weakly dislocated Miocene volcanics occur within the Malka–Petropavlovsk zone of transverse dislocations and overlie the Cretaceous island-arc complexes (Fig. 1). Thus, the early Miocene age of the volcanic rocks of the Pribrezhny complex as well as their low degree of deformation compared to the Kronotsky terrane complexes raises the issue of the tectonic affiliation of these volcanics and their geodynamic position.

This work describes the detailed paleomagnetic studies of magmatic formations conducted in southern Kamchatka. The main objectives of our research were (1) to obtain a reliable paleomagnetic pole for the Miocene, which can be used in paleotectonic reconstructions of the northwestern Pacific; (2) to determine the paleolatitude of the formation of the Pribrezhny complex volcanics and their temporal correlation with the last phase of deformations; and (3) to typify

the volcanics by age and identify the main magmatic events.

2. GEOLOGY OF THE REGION AND STUDY OBJECTS

The volcanic bodies of the Pribrezhny complex compose the coastal ridges of the southern Kamchatka Pacific coast. Stratified formations are represented by tuff sequences and, less frequently, lava flows. Among the subvolcanic bodies, thin (up to 5–8 m thick) dikes are predominant; sills and larger stock-like massifs are also present. The largest intrusion in the study area is the Akhomten granite massif, which is attributed to the Miocene plutonic complex of the same name (Slyadnev et al., 2006). The Miocene magmatites have extremely diverse petrographic compositions, forming a continuous series from basalts and picrobasalts to rhyolites.

The volcanics of the Pribrezhny complex and the granitoids of the Akhomten massif are hosted by the volcanic-terrigenous deposits of the Presnovskaya (Eocene), Zhirovskaya (Oligocene), Mutnovskaya (Oligocene–Miocene), and Asacha (Miocene) formations (Slyadnev et al., 2006). These deposits are relatively weakly dislocated, crumpled into gentle folds with dip angles of up to 25°–30° or form isolated monoclines between volcanic formations. These deformations can probably be partly synmagmatic and associated with intrusion of nearby intrusive bodies.

During this study, we have sampled stratified and intrusive bodies in several regions on the Pacific coast of southern Kamchatka (Bergal-Kuvikas et al., 2022) (Fig. 1). The sampled bodies, from south to north, are briefly described below.

(1) Five andesitic intrusive bodies were sampled in the Mutnaya Bay area. These are the steeply dipping, northwesterly striking dikes with a thickness of 1.5–8 m (sites 8.1-22, 8.2-22, 9-22, 12-22) and a subvolcanic body of unclear morphology (site 10-22). The intrusions cut the sandstones and conglomerates of the Asacha formation crumpled into gentle folds.

(2) In Russkaya Bay and Cape Kekurnyi area, granodiorites (sites 19-22, 21-22, 24-22) and monzodiorites (20-22, 22.2-22) of the Akhomten massif were sampled. According to field observations and literature data (Slyadnev et al., 2006), monzodiorites correspond to the first phase, and granodiorites to the second phase of the Akhomten complex. Also sampled were subvertical dikes of porphyritic basalts (sites 22.1-22, 23-22) cutting the Akhomten massif.

(3) In the Vilyuchinskaya Bay, samples were taken from dikes of granosyenite porphyries (sites 3-22, 5-22), basalts (4-22), and flow-banded rhyolites (2-22). All dikes are thin (0.5–3 m), with strike varying from northwest to almost meridional. The hosting rocks are sandy-gravelly deposits of the Mutnovskaya Formation, dipping northeast at angles ranging from 20° to 50°. Subhorizontal, felsic, locally ignimbrite-like tuffs (sites 18-22) are also sampled in the neighboring Sabotazhnaya Bay.

(4) On the Starichkov Island and in the Malyi Vilyui River mouth, subvolcanic bodies of basaltic–andesitic composition with complex morphology were sampled from sites 14-22 to 17-22. Samples were also taken from gently dipping gravelly sandstones of the Presnovskaya Formation (site 13-22) 25 m west of the contact with the subvolcanic body.

(5) In the vicinity of Vilyuchinsk, subvolcanic bodies and lava flows of basaltic andesite composition (sites 7-21–13-21, v3-23) and rhyolite sills (6-21, v2-23) were sampled. Host rocks are gently folded volcanic-sedimentary deposits of the Pribrezhny complex.

(6) South of Petropavlovsk-Kamchatsky, in the region of Zavoiko Peninsula, samples were taken from lava flows (sites 16-21, 27-21) and mafic dikes (14-21, 17.1-21, 18.2-21), as well as from gabbro massifs (17.2-21, 18.1-21, 18.3-21, 21-21) attributed to the Pribrezhny complex. The dikes cut through the gabbroid massifs and probably represent the youngest episode of magmatism in this location.

(7) North of the Vilyuchinsky volcano, in the Paratunka River valley, samples were collected from two felsic subvolcanic bodies of dyke-like morphology (sites 3-23, 4-23), located in the field of terrigenous deposits of the Mutnovskaya Formation.

3. METHODS

Paleomagnetic samples were collected manually or using a mechanical sampler. Their orientation in space was determined using a magnetic compass with constant monitoring of the probable influence of strongly magnetic rocks on the compass needle. Eight to 25 oriented samples were acquired from each site. The local magnetic declination was calculated from the IGRF model (https://geomag.bgs.ac.uk/data_service/models_compass/igrf_calc.html). Laboratory paleomagnetic studies and processing of demagnetization data were performed in the Laboratory of the Main Geomagnetic Field and Rock Magnetism of Schmidt Institute of Physics of the Earth of the Russian Academy of Scieces (IPE RAS). All samples were subjected to stepwise thermal demagnetization up to complete magnetization removal (10–16 steps), which was achieved in most cases at temperatures of 500–620°C. Samples were demagnetized in non-magnetic MMTD-80 thermal demagnetizers with a residual field of at most 5–10 nT. The remanent magnetization of the samples was measured using a JR-6 (AGICO) spin magnetometer and a 2G Enterprises cryogenic magnetometer. In addition to thermal demagnetization, part of the samples was subjected to demagnetization by alternating magnetic field (AF) using a demagnetization unit built into the cryogenic magnetometer. AF demagnetization was conducted up to

130 mT. The remanent magnetization measurements were processed using the Enkin software package (Enkin, 1994) with PCA method (Kirschvink, 1980) to isolate the remanence components. The obtained data were analyzed based on Fisher's statistics (Fisher, 1953). The angular difference between the poles was calculated in the PMCALC program of the Enkin package (Enkin, 1994) with uncertainties taken into account according to (Debiche and Watson, 1995).

The temperature dependence of magnetic susceptibility K(T) was measured on MFK-1FA kappabridge with CS-3 high-temperature furnace apparatus with heating to 700°C (in air) and subsequent cooling to room temperature. Hysteresis loops were recorded on a RMS MicroMag 3900 vibration magnetometer at room temperature with a saturation field of 1 T. The domain structure of ferromagnetic grains was evaluated from the Day–Dunlop diagram (Day et al., 1977; Dunlop, 2002). Microscopic studies were conducted on a TESCAN MIRA LMS scanning electron microscope with an Ultim Max 65 energy dispersive X-ray (EDX) spectrometer with integrated AZtecLive Automated software (Oxford Instruments) at IPE RAS Center of Shared Research Facilities (CSRF) "Petrophysics, Geomechanics and Paleomagnetism" in Moscow (Veselovskiy et al., 2022).

4. MAGNETIC MINERALOGY

To characterize the composition of the main magnetic minerals and evaluate the possibility of preservation of primary remanent magnetization, rock magnetic studies were conducted on selected samples representing magmatic bodies of different composition and different paleomagnetic record.

The electron microscopic studies revealed a variety of magnetic mineral structures. Primarily magmatic magnetite and/or titanomagnetite crystals were detected in all studied samples. Both large homogeneous unaltered grains (Fig. 2a) and magnetite crystals with ilmenite lamellae characteristic of high-temperature deuteric oxidation (Haggerty, 1976; McEnroe, 1996) (Figs. 2b, 2e) are widespread. In a number of samples, large or small titanomagnetite grains are cut by cracks, indicating single-phase oxidation processes (Gapeev and Tselmovich, 1989) (Fig. 2c). In the granodiorites of the Akhomten massif (sites 19-22), as well as in basalt dikes and lava flows (sites 10-21, 16-21), primary magmatic inclusions of titanomagnetite and magnetite were found in pyroxenes and amphiboles (Fig. 2d). Thus, in most of the studied samples, the structures of magnetic minerals suggest their magmatic origin and possible preservation of primary thermoremanent magnetization. Felsic volcanics (site 6-21) proved to be most altered, as indicated by the presence of secondary aggregates of magnetite and albite, along with clusters of secondary pyrite within the groundmass (Fig. 2f).

The temperature curves of magnetic susceptibility in most cases show the predominance of magnetite or low-Ti titanomagnetite with Curie temperatures of 570–590°C among the magnetic minerals (Figs. 3a–3c). After the heating and cooling cycles, the magnetic susceptibility is frequently observed to decrease, which is probably due to partial oxidation of magnetite. The curves of a number of samples also have a "tail" above temperatures of 600°C due to the presence of hematite or a significant proportion of the paramagnetic component. The flat peak around 300°C observed in the heating curves of some samples (Fig. 3c) can be related to the presence of maghemite and its subsequent oxidation to hematite (Liu et al., 2005).

Rhyolites (site 6-21) differ sharply from all studied samples by their low bulk magnetic susceptibility (for most samples $0.1–1 \times 10^{-3}$ SI units, compared to $1–50 \times 10^{-3}$ for basic and intermediate rocks). After heating to 700°C, the cooling curves show a sharp growth in magnetic susceptibility (Fig. 3d), which is associated with the formation of magnetite from pyrite. The instability of felsic volcanics to heating, coupled with the presence of secondary magnetite and sulfides, explains the generally low quality of the paleomagnetic signal in these rocks (see Section "Paleomagnetism").

The hysteresis parameters M_{rs}/M_s and H_{cr}/H_c for the studied samples vary widely (0.002–0.3 and 1.5–7, respectively). Samples from different regions form different clusters in the Day-Dunlop diagram (Fig. 3e), reflecting changes in the composition and structure of the rocks and variations in the domain state of the magnetic grains. Most of the basite samples from the vicinity of Vilyuchinsk and the Zavoiko Peninsula fall in the field corresponding to pseudo-single-domain (PSD) magnetite and titanomagnetite grains, which is typical for samples from volcanic rocks and shallow intrusions of basic composition (e.g., (Latyshev et al., 2021; 2023)). Samples of volcanics from the vicinity of Vilyuchinsk are characterized by the highest M_{rs}/M_s ratios in the range of 0.1–0.3, suggesting a high proportion of single-domain (SD) particles. Samples of porphyritic andesites from the Mutnaya Bay and granitoids from the Akhomten massif have maximum H_{cr}/H_c ratios, tending toward the field of multidomain (MD) grains, which indicates larger magnetite grain sizes.

5. PALEOMAGNETISM

The quality of the paleomagnetic signal in the studied volcanics varies from excellent to practically uninterpretable. Nevertheless, at all sites considered in this work, it was possible to identify characteristic remanence components from a sufficient number of samples and calculate mean paleomagnetic directions. The results of stepwise thermal demagnetization and AF demagnetization are consistent with each other,

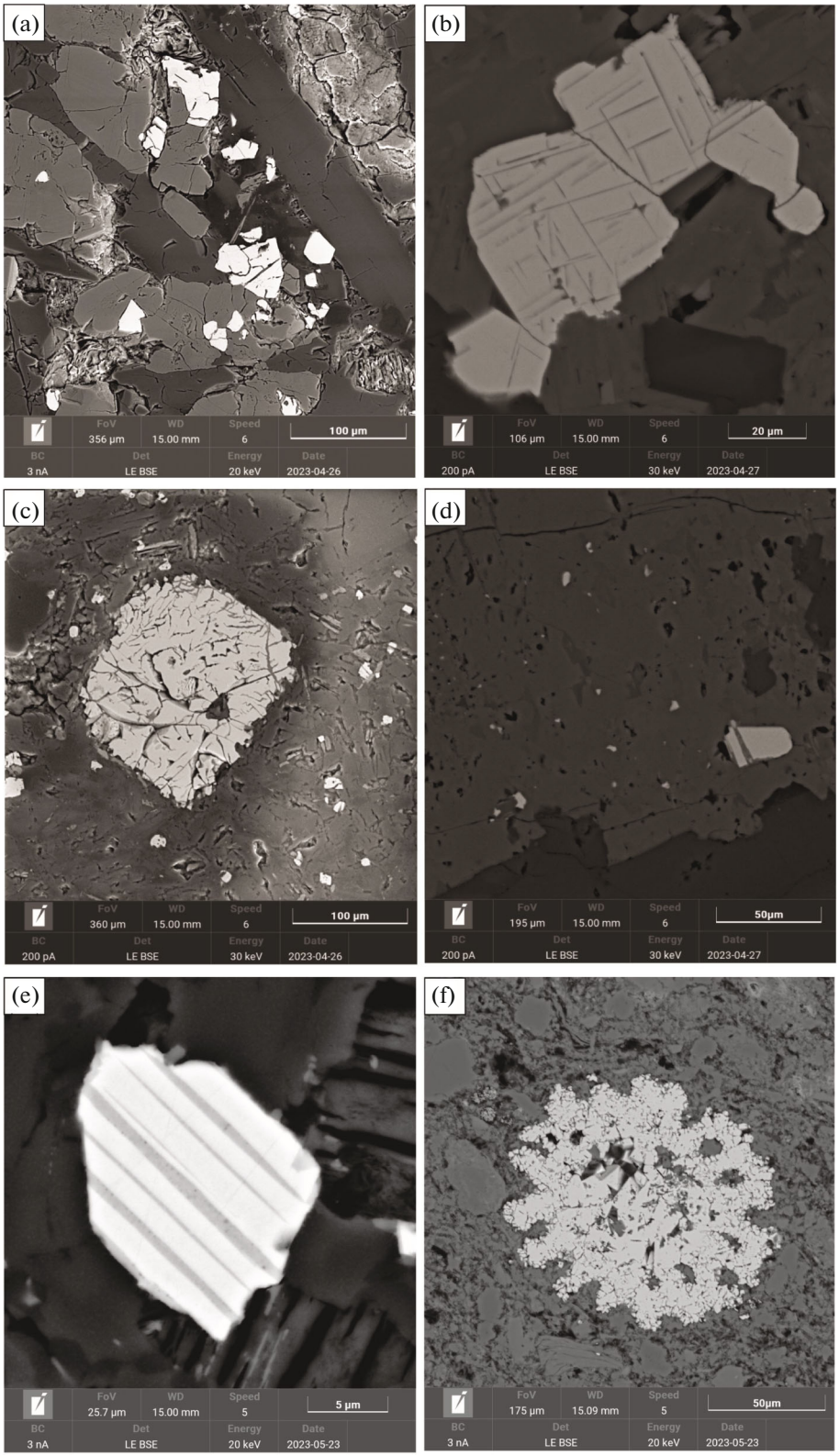

Fig. 2. Electron microscopic images of magnetic minerals in studied magmatic rocks: (a) homogeneous unaltered titanomagnetite crystals in gabbro, site 17.2-21; (b) magnetite grains with high-temperature deuteric oxidation structures, granodiorites, site 19-22; (c) large magnetite grain with single-phase oxidation structures, andesite dike, site 10-22; (d) primary magmatic magnetite inclusions in amphibole, granodiorites of Akhomten massif, site 19-22; (e) magnetite with ilmenite lamellae in gabbro, site 21-21; (f) pyrite clusters in rhyolites, site 6-21.

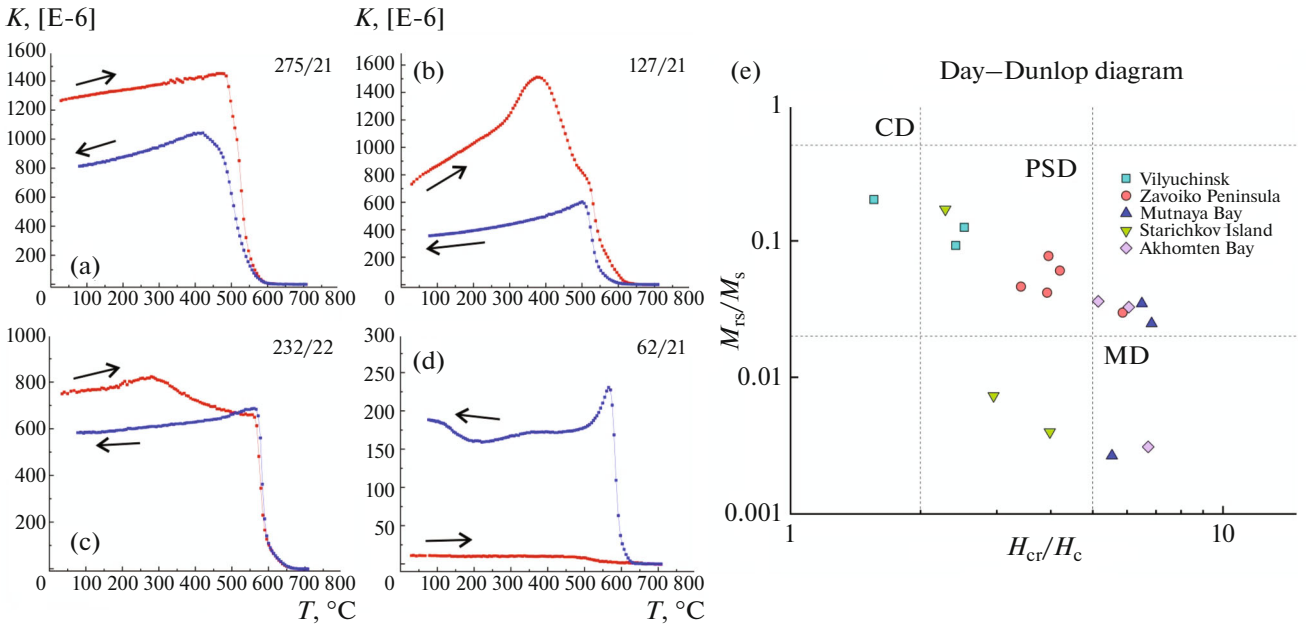

Fig. 3. Magnetic properties of studied samples. (a)–(d) Thermal curves of magnetic susceptibility: (a) site 21-21, gabbro; (b) site 11-21, andesites; (c) site 19-22, granodiorites; (d) site 6-21, rhyolites. (e) Day–Dunlop diagram (Day et al., 1977; Dunlop, 2002). M_s is saturation magnetization, M_{rs} is saturation remanent magnetization, H_c is coercive force, H_{cr} is remanent coercive force. Fields in diagram: SD, single-domain grains; PSD, pseudo-single-domain grains; MD, multi-domain grains.

with AF demagnetization providing better quality of the paleomagnetic record in most cases. Most sites are characterized by a two-component remanence composition (a few exceptions are described below). The low-temperature and low-coercive remanence components are removed at 200–300°C and 5–10 mT and frequently have directions close to the present field. This component is most likely to have viscous nature and is not discussed below. The high-temperature and high-coercive components are isolated in different field and temperature intervals and are characterized by a variety of directions, but in most cases they come to the origin of coordinates in the Zijderveld diagrams (Zijderveld, 1967). Next, we consider the features of the paleomagnetic record for magmatic bodies from different sampling regions.

The andesites of Mutnaya Bay, as a rule, have a single stable high-temperature and high-coercive magnetization component (Fig. 4d), which is removed in the temperature interval of 400–560°C (rarely from 350 to 600°C) and in the fields of 20–110 mT (sometimes up to 130 mT). Site-mean paleomagnetic directions for all dikes correspond to normal polarity and have north or northwest declinations.

The granitoids of the Akhomten massif and the basalt dikes cutting them are characterized by a diverse paleomagnetic signal. In most cases, a single stable component is isolated in the intervals 350–580°C and 20–130 mT (Fig. 4c). This component has normal polarity at sites 19-22, 20-22, 22.2-22, 24-22 (granodiorites and monzodiorites) and a reversed polarity at sites 21-22 (granodiorites), 22.1-22, and 23-22 (basaltic dikes). Thus, the formation of the Akhomten massif covers at least two intervals of normal and reversed polarity. It is worth noting that normally magnetized monzodiorites (site 22.2-22) are cut by a reversely magnetized dike (22.1-22), which indicates the absence of magnetic overprint in this area. A similar situation is observed at site 23-22, where the only granodiorite sample taken directly from the exocontact zone of the dike is magnetized in reversed polarity, while granodiorite samples taken 10 cm or more apart (site 23-22e) show normal polarity and bear no traces of remagnetization. Overall, the data for sites 22-22 and 23-22 indicate the absence of regional remagnetization and provide a positive baked contact test.

The sampled bodies in the Vilyuchinskaya Bay region generally have a noised paleomagnetic signal of only moderate quality. The most stable component is isolated in the intervals of 350–560°C (sometimes up to 600°C) and 8–130 mT. This component corresponds to normal polarity at site 2-22 (subvolcanic rhyolites) and to reversed polarity at the other sites. Also, at sites 4-22 and 18-22, a medium-temperature/medium-coercive component (up to 500°C or up to 20 mT) of normal polarity is identified in a number of samples (Fig. 4a). This component can be related to remagnetization by more recent magmatic events or to viscous magnetization.

Basaltoids from the subvolcanic bodies in the region of the Starichkov Island have a clear paleomagnetic record in most samples (Fig. 4b). In addition to

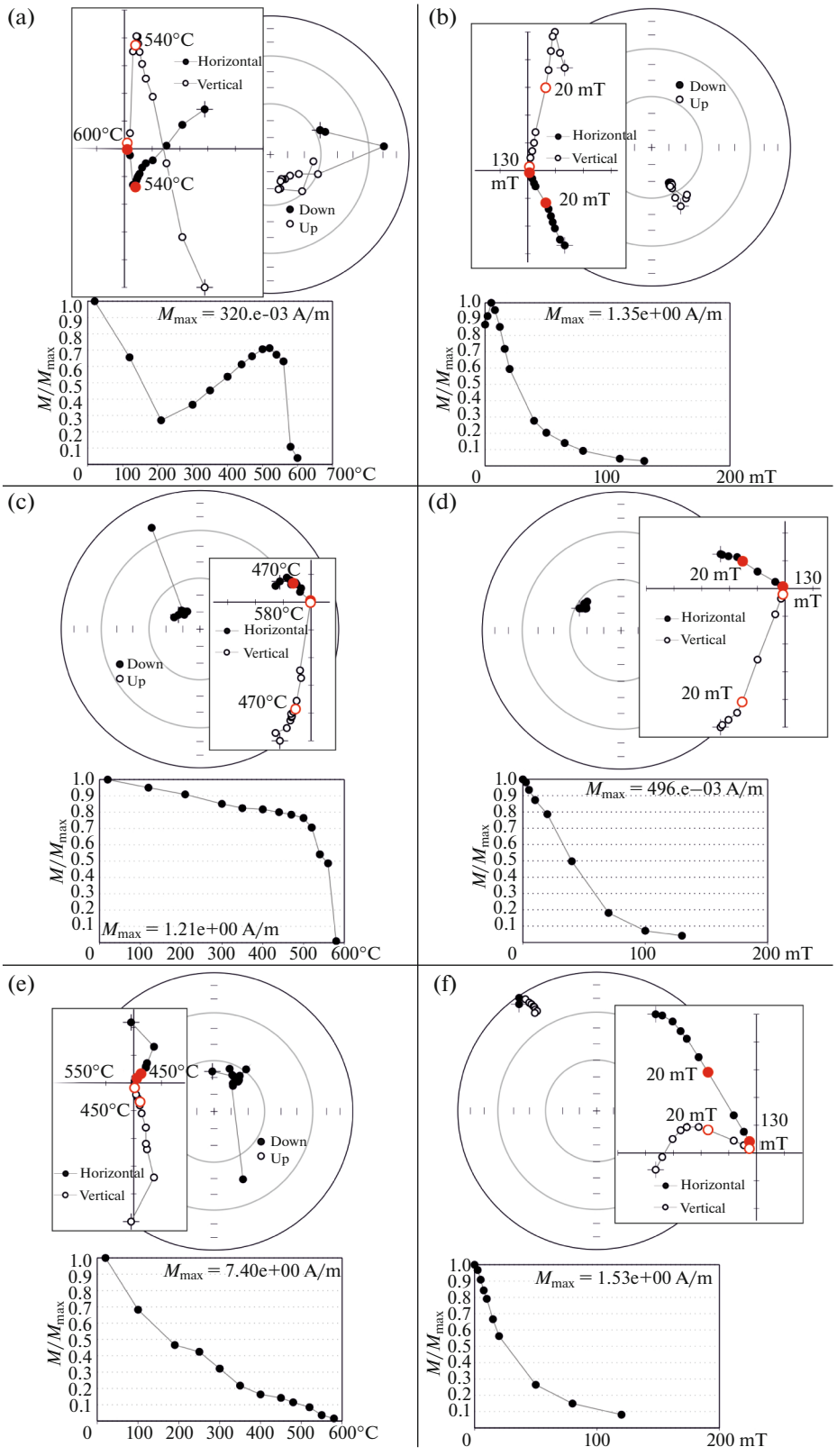

Fig. 4. Thermal and AF demagnetization results: (a) sample 219, site 18-22 (rhyolite tuffs); (b) sample 193, site 16-22 (andesites); (c) sample 241, site 20-22 (monzodiorites); (d) sample 151, site 12-22 (andesites); (e) sample 195, site 17.2-21 (dolerites); (f) sample 181, site 7-21 (basalts). Stratigraphic coordinate system.

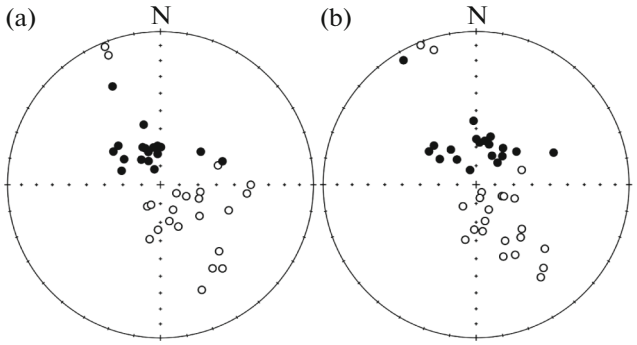

Fig. 5. Distribution of site-mean paleomagnetic directions: (a) geographic coordinate system; (b) stratigraphic coordinate system. Filled and open circles correspond to normal and reversed polarity.

the low-temperature/low-coercive viscous component, they have a single stable component isolated in the intervals 440–600°C and 20–110 mT. The mean paleomagnetic directions over all sites are characterized by southeasterly declinations and negative inclinations. The remanence of the terrigenous deposits of the Presnovskaya Formation (sites 13-22), sampled 25 m from the contact of subvolcanic bodies, corresponds to normal polarity (exception for a single sample), which indicates the absence of regional remagnetization.

The magmatic bodies sampled in the vicinity of Vilyuchinsk are extremely diverse in the pattern of paleomagnetic record and in the calculated paleomagnetic directions. The clearest paleomagnetic signal is identified in subvolcanic bodies of basaltic composition (sites 7-21, v3-23) (Fig. 4f), while the poorest quality of the paleomagnetic signal is observed in sills of rhyolite composition (sites 6-21, v2-23). Felsic subvolcanic bodies from the Paratunka River valley (sites 3-23, 4-23) are also characterized by noisy records and instability during thermal demagnetization. Most of the sampled bodies are magnetized in reversed polarity (rhyolites from sites 6-21, v2-23, andesites from sites 8-21, 10-21, 13-21, and basalt dikes at site v3-23). Normal polarity is established in felsic subvolcanoes from the Paratunka River valley (sites 3-23, 4-23), dikes, and andesite lava flows (sites 11-21, 12-21). Site 7-21 differs from others by its anomalous paleomagnetic directions with northwestern declinations and nearly zero inclinations.

In the region of the Zavoiko Peninsula, most sites have a single stable magnetization component, which is unblocked in the temperature interval of 400–600°C (rarely up to 640°C) and in the fields of 20–120 mT (Fig. 4e). For four sites (17.2-21, 18.1-21, 18.3-21, 21-21), the calculated mean paleomagnetic directions have a reversed polarity with southeastern declinations. At three sites representing dolerite dikes cutting the more ancient magmatic bodies (14-21, 17.1-21, 18.2-21), the characteristic remanence component has normal polarity. Finally, for two sites represented by basalts and basaltic andesites (16-21, 27-21), the mean directions are anomalous and close to those for the above site 7-21 in the stratigraphic coordinate system. It should be emphasized that the dolerite dikes 17. 1-21 and 18.2-21, which have normal polarity, cut through the reversely magnetized gabbroid massifs (sites 17.2-21, 18.1-21, 18.3-21), indicating the absence of regional remagnetization in this region.

6. DISCUSSION

The analysis of the distribution of site-mean directions reveals three directional groups among all objects (Fig. 5, Table 1). These groups are as follows.

(1) The group of reversed polarity directions with southeastern declinations. This group includes mean directions over 21 sites representing magmatic bodies of different compositions (from basalts to rhyolitic tuffs) from various regions.

(2) The group of normal polarity directions with northern and northwestern declinations. This group consists of 18 sites, also of diverse composition.

(3) The group of three sites with paleomagnetic directions not typical for the Cenozoic of Kamchatka. In the stratigraphic coordinate system, the directions are closely grouped, characterized by northwestern declinations and inclinations close to zero.

We excluded from further calculations the terrigenous rocks of the Presnovskaya Formation (site 13-22) due to their Eocene age, granodiorites from the exocontact of the basalt dike due to the small number of samples (site 23-22e), and rhyolites from the vicinity of Vilyuchinsk (sites 6-21, v2-23), characterized by a noisy paleomagnetic signal, an abundance of secondary magnetic phases, and inclinations that are too low compared to the main group. We also excluded sites 4-23, 8.2-22, and 21-21 because their paleomagnetic directions differ significantly from all other sites, perhaps due to the uncertainties of tilt correction.

The paleomagnetic directions of group 1 (reversed polarity) are characterized by higher concentration in the stratigraphic coordinate system than in the geographic system (Ks = 24.3, Kg = 13.7; $\alpha 95s = 7.2°$, $\alpha 95g = 9.7°$). This favors the formation of most of the reversely magnetized magmatic bodies before the main deformation phase. The maximum concentration is achieved at 102% unfolding (Watson and Enkin, 1993).

The normal-polarity directions (group 2), on the contrary, are tightly grouped in the geographic coordinate system (Kg = 65.3, Ks = 31.1; $\alpha 95g = 4.8°$, $\alpha 95s = 7.0°$), forming a cluster with predominantly northwestern declinations. It should be noted that this group includes a number of basaltic dikes from the region of the Zavoiko Peninsula, which cut the more ancient reversely magnetized magmatic bodies and are probably the youngest ones among the magmatic

Table 1. Site-mean paleomagnetic directions. *N*, number of samples (number of sites is shown in bold); Dg(s)/Ig(s), declination/inclination in geographic (stratigraphic) coordinate system; *K*, concentration parameter; α95, confidence angle (in stratigraphic coordinate system for mean directions for groups 1 and 3, in geographic coordinate system for mean directions for group 2). Sampling regions: A, Russkaya Bay, Akhomten Massif; B, Vilyuchinsk; Vil, Vilyuchinskaya Bay; Z, Zavoiko Peninsula; M, Mutnaya Bay; P, Paratunka river valley; S, Starichkov Island and Bolshoy Vilyui river mouth

Site	*N*	Dg	Ig	Ds	Is	*K*	α95	Composition	Morphology of a body	Sampling region	Coordinates
1. Reversed polarity directions											
22.1-22	7	110.4	−68.1	110.4	−68.1	135.4	5.2	Basalt	Dike	A	N 52°26.191′ E 158°30.372′
23-22	5	114.9	−74.9	114.9	−74.9	224.8	5.1	Basalt	Dike	A	N 52.43556° E 158.50486°
21-22	12	153.6	−74.9	153.6	−74.9	112.8	4.1	Granodiorite	Massif	A	N 52.41692° E 158.45945°
10-21	9	129.1	−63.1	146	−84.8	59.2	6.7	Andesite	Dike	V	N 52.87120° E 158.60281°
13-21	9	182.3	−65.7	182.3	−65.7	64.4	6.5	Andesite	Flow	V	N 52.91267° E 158.55848°
8-21	7	191.2	−60	191.2	−60	32.6	10.7	Basalt	Dike	V	N 52.87120° E 158.60281°
v3-23	11	210.8	−76.3	210.8	−76.3	98.3	4.6	Basalt	Dike	V	N 52.86733° E 158.58400°
6-21	9	158.6	−26.8	145.2	−26.8	14.5	14	Rhyolite	Sill	V	N 52.82489° E 158.59835°
v2-23	21	148.2	−35.6	133.2	−38.3	32.5	5.7	Rhyolite	Sill	V	N 52.82497° E 158.59792°
4-22	10	96.1	−42.6	140.6	−52.9	46.9	7.1	Basalt	Dike	Vil	N 52.63457° E 158.41003°
3-22	22	110.9	−50.5	159.4	−48.1	87.9	3.3	Granosienite Porphyry	Dike	Vil	N 52.63518° E 158.40365°
5-22	9	90.4	−41	134.4	−55.6	39.1	8.3	Granosienite Porphyry	Dike	Vil	N 52.63457° E 158.41003°
18-22	8	166.4	−69.8	166.4	−69.8	88	5.9	Rhyolite tuff	Blanket	Vil	N 52.64498° E 158.54825°
18.1-21	5	138.8	−41.4	153.1	−55.9	31.8	13.8	Gabbro	Massif	Z	N 52.95951° E 158.64906°
18.3-21	3	138.7	−41.3	152.9	−55.8	77.2	14.1	Gabbro	Massif	Z	N 52.95951° E 158.64906°

Table 1. (Contd.)

Site	*N*	Dg	Ig	Ds	Is	*K*	α95	Composition	Morphology of a body	Sampling region	Coordinates
21-21	5	204.6	−78	141.1	−30.5	33.1	13.5	Gabbro	Massif	Z	N 52.91235° E 158.68523°
17.2-21	7	143.6	−32.2	150.5	−45.9	16.7	15.2	Dolerite	Massif	Z	N 52.95929° E 158.64600°
14-22	13	71.9	−57.5	72.8	−64.5	59.8	5.4	Basaltic andesite	Subvolcano	S	N 52.78943° E 158.57071°
15-22	9	100.8	−68.4	113.8	−73.9	556.7	2.2	Basaltic andesite	Subvolcano	S	N 52.78851° E 158.57102°
16-22	14	157.1	−65.5	172.1	−64.6	242.3	2.6	Basaltic andesite	Subvolcano	S	N 52.77861° E 158.61442°
17-22	16	119.4	−80.3	165	−82.4	229.6	2.4	Basaltic andesite	Subvolcano	S	N 52.77977° E 158.61505°
	18	**129.7**	**−64.8**	**150.1**	**−68**	**24.3**	**7.2**	**Group 1 mean without excluded directions**			
2. Normal polarity directions											
19-22	12	322.6	73.2	322.6	73.2	104.4	4.3	Granodiorite	Massif	A	N 52.41623° E 158.54909°
24-22	9	344.4	56.5	357.7	55.7	34.3	8.9	Granodiorite	Massif	A	N 52.45869° E 158.49140°
23-22e	3	258.0	79.1	258.0	79.1	41.5	19.4	Granodiorite	Dike exocontact	A	N 52.43556° E 158.50486°
20-22	10	337.5	81.6	337.5	81.6	153	3.9	monzodiorite	Massif	A	N 52.40504° E 158.54683°
22.2-22	9	305.1	66.3	305.1	66.3	84.6	5.6	Monzodiorite	Massif	A	N 52°26.191′ E 158°30.372′
11-21	4	333.3	75.9	44.3	73.7	93.3	9.6	Andesite	Flow	V	N 52.87120° E 158.60281°
12-21	5	354.3	70.3	36.4	65.8	75	8.9	Andesite	Dike	V	N 52.87120° E 158.60281°
2-22	21	312.8	59.2	312.8	59.2	171.6	2.4	Rhyolite	Dike	Vil	N 52.65224° E 158.41232°
14-21	5	305.2	59.1	305.2	59.1	41.1	12.1	Basalt	Dike	Z	N 52.95214° E 158.65018°

Table 1. (Contd.)

Site	*N*	Dg	Ig	Ds	Is	*K*	α95	Composition	Morphology of a body	Sampling region	Coordinates
17.1-21	6	334.6	67.9	28.8	72.5	79.6	7.6	Diabase	Dike	Z	N 52.95929° E 158.64600°
18.2-21	6	349.3	69.8	42.8	69.4	51.6	9.4	Diabase	Massif	Z	N 52.95951° E 158.64906°
8.1-22	11	354.8	73.6	17.9	67.5	110.3	4.4	Andesite	Dike	M	N 52.22713° E 158.39368°
8.2-22	10	69.3	54.3	67.6	44.4	40.5	7.7	Andesite	Subvolcano	M	N 52.22713° E 158.39368°
9-22	11	358.6	69.4	16.8	63.2	198.4	3.2	Andesite	Dike	M	N 52.23002° E 158.40350°
10-22	16	339.7	71.4	4.7	67.5	130	3.2	Andesite	Dike	M	N 52.22989° E 158.40409°
12-22	10	337.4	69	0.3	65.7	159.5	3.8	Andesite	Dike	M	N 52.22934° E 158.40490°
3-23	11	289.8	68	324.2	67	34.6	7.9	Rhyolite	Dike	P	N 52.73838° E 158.25307°
4-23	5	50.7	62.1	50.7	62.1	173.1	5.8	Rhyolite	Subvolcano	P	N 52.81394° E 158.21406°
13-22	12	355.7	69.2	11.2	66.2	20.4	9.8	Sandstone	Presnovskaya Formation	S	N 52.79012° E 158.56942°
	15	**330.3**	**70**	**354**	**70.8**	**65.3**	**4.8**	**Group 2 mean without excluded directions**			
3. Group of anomalous directions											
7-21	16	334	29.3	329.7	6.6	104.4	3.6	Basalt	Subvolcano	V	N 52.89639° E 158.62985°
16-21	9	338	−10.1	342.5	−9	20.7	11.6	Basalt	Flow	Z	N 52.95446° E 158.65054°
27-21	10	338.2	−2.6	338.2	−2.6	69.9	5.8	Basalt	Flow	Z	N 52.95012° E 158.68228°
	3	**336.8**	**5.4**	**336.8**	**−1.7**	**63.5**	**15.6**	**Group 3 mean**			
	33			**330.2**	**68.9**	**34.8**	**4.3**	**Groups 1 and 2 mean**			

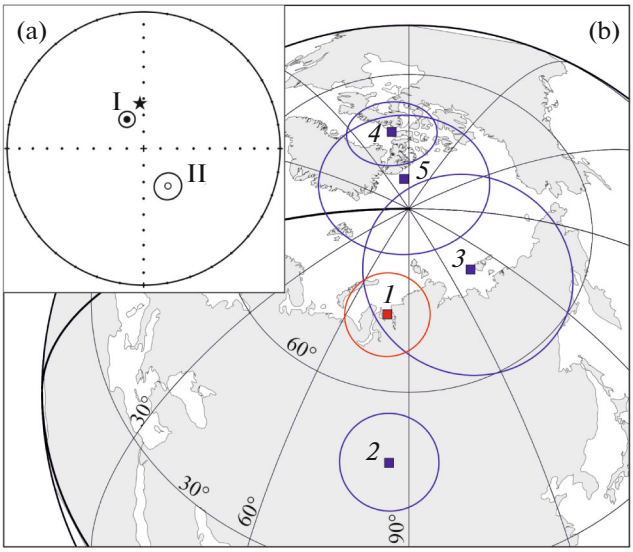

Fig. 6. (a) Mean directions for directional groups: I, normal polarity, geographic coordinate system; II, reversed polarity, stratigraphic coordinate system. Asterisk indicates present geomagnetic field direction; (b) paleomagnetic pole for Miocene of southern Kamchatka and its comparison with published data: *1*, mean pole for Miocene volcanics of Pribrezhny complex (this work); *2*–*5*, results of previous studies: *2*, Eocene, Kronotsky terrane (Levashova et al., 2000); *3*, Eocene–Oligocene, Ilpinsky Peninsula (Kovalenko, 1992); *4*, Eocene, Kronotsky terrane (Pechersky et al., 1997); *5*, Oligocene–Miocene, Western Kamchatka (Kazansky et al., 2021).

complexes considered in this work. This suggests that at least part of the normally magnetized bodies could have formed after the termination of the main phase of tectonic activity and have did not experienced significant tectonic deformations. Although remagnetization of individual bodies cannot be ruled out completely, the secondary origin of the post-folding remanence seems unlikely, since in a number of cases the normally magnetized dikes (sites 17.1-21 and 18.2-21) cut the reversely magnetized bodies. Since we cannot separate the normally magnetized post-folding bodies from the pre-folding ones for certain, the subsequent calculations for normally magnetized bodies are conducted with paleomagnetic directions in the geographic coordinate system.

The mean paleomagnetic directions for the normal polarity group in situ and for the reversed polarity group in the stratigraphic coordinate system (Fig. 6a) are antipodal: $\gamma/\gamma_{cr} = 2.0°/6.5°$. The reversal test according to (McFadden and McElhinny, 1990) is positive and corresponds to class B. Here, the mean directions calculated for both groups 1 and 2 in the stratigraphic coordinate system are not antipodal: $\gamma/\gamma_{cr} = 7.9°/7.5°$. This supports our version of using normal polarity paleomagnetic directions in the geographic coordinate system. The positive reversal test indicates that the secular variation of the geomagnetic field is averaged and that there is no significant contribution from the secondary remanence components formed after the intruding of the magmatic bodies.

Thus, the primary nature of remanent magnetization for groups 1 and 2 is favored by the following arguments:

(1) positive baked contact test for a number of objects (see section "Paleomagnetism");

(2) positive fold test for reversely magnetized bodies;

(3) positive reversal test for mean directions in groups 1 and 2;

(4) the presence of primary magmatic magnetic minerals that can preserve thermoremanent magnetization (see section "Magnetic Mineralogy").

However, although the above signs suggest an absence of a regional remagnetization event, it cannot be ruled out that individual sampled bodies were remagnetized during subsequent magmatic events.

As far as it concerns group 3, the paleomagnetic directions that are anomalous for the Cenozoic of Kamchatka cannot be explained by local remagnetization or rock composition peculiarities, since this group includes spatially distant sites representing bodies of different composition and morphology. The paleomagnetic record or rock magnetic characteristics also lack any evident peculiarities that could distinguish these sites from the ones with normal directions. As of now, the anomalous directions of this group can be explained by the specific state of the geomagnetic field at the time of the formation of magmatic bodies (e.g., an excursion) or by incorrect consideration of the structural position of the bodies. One possible interpretation is the rotation of blocks in the fault zones around a horizontal axis, as indicated by the elongation of the cloud of directions along a great circle arc in the geographic coordinate system (Fig. 5a). This scenario appears to be plausible, given the location of group 3 sites within the Malka–Petropavlovsk transverse fault zone. However, the absence of structural evidence such as fault dislocations of the corresponding orientation and steeply dipping host rocks does not allow this interpretation to be accepted. Group 3 sites were excluded from the subsequent calculations.

The calculated paleomagnetic directions show that the magmatic bodies were formed during several intervals of normal and reversed polarity of the geomagnetic field. Although it is not possible to determine the exact number of these intervals, it is most likely that there were at least three. This is suggested by the observed structural relationship between the bodies of different polarities. Specifically, within the Akhomten massif, the reversely magnetized dikes cut through granitoids that have normal polarity, while in the region of the Zavoiko Peninsula, the normally magnetized basalt dikes cut through more ancient intrusions of reversed polarity.

Table 2. Paleomagnetic poles for Paleogene-Neogene formations in Kamchatka and southern Koryakia. *N*—number of samples or sites; Plat/Plong—latitude/longitude of the paleomagnetic pole; A95—radius of the circle of confidence; γ/γ_{cr}—angular difference with the pole for the Pribrezhny complex/critical angle

Object	Age, Ma	*N*	Plong, deg	Plat, deg	A95, deg	Paleolatitude, deg	γ/γ_{cr}, deg	Data source
Kamchatsky Mys Peninsula, Kronotsky terrane	46–43	54	280.1	74.5	7.1	47	32.7/7.3	Pechersky et al., 1997
Kronotsky Peninsula, Kronotsky terrane	42–38	8	85.3	48.8	7.8	45.1	23.1/7.5	Levashova et al., 2000
Ilpinsky Peninsula, Achaivayam-Valaginskaya Arc	39–29	40	113.9	68.8	12.8	67	10.8/10.1	Kovalenko, 1992
Kvachina Bay, West Kamchatka	38–23	93	277.8	84.4	13.5	54.6	22.9/9.4	Kazansky et al., 2021
Pribrezhny complex, Southern Kamchatka	19–13	33	79	72	6.7	52.3		This work

To calculate the mean pole characterizing the Miocene volcanics of southern Kamchatka, we used data from 15 sites of normal polarity (in the geographic coordinate system) and 18 sites of reversed polarity (in the stratigraphic coordinate system). In addition to the anomalous directions of group 3, a number of normal and reversed polarity sites indicated above were also excluded from the final calculation.

The mean paleomagnetic pole calculated over 33 sites has the coordinates Plat = 72.0°, Plong = 79.0°, A95 = 6.7°. The averaging of secular geomagnetic variation recorded in the sampled bodies is provided by (1) the covered age range of 5.9 Ma, according to isotopic K-Ar dating; (2) the presence of remanence directions corresponding to opposite polarities and a positive reversal test; (3) the absence of an anomalously tight grouping of paleomagnetic directions (the concentration parameter for the mean direction over the 33 sites is 34.8), which could indicate a geologically ultra-rapid formation of magmatic bodies (e.g., (Konstantinov et al., 2014; Latyshev et al., 2018)).

The calculated paleomagnetic pole corresponds to a paleolatitude of 52.3°, which is comparable with present latitude of the sampled magmatic formations (52.2°–53.0°). This indicates that southern Kamchatka has not experienced significant latitudinal displacements after the formation of the Pribrezhny complex, i.e., after the early Miocene.

The paleomagnetic pole calculated for the Pribrezhny volcanic complex differs significantly from the published poles for the Eocene-Oligocene of Kamchatka and southern Koryakia (Kovalenko, 1992; Pechersky et al., 1997; Levashova et al., 2000). This is quite expected due to the significantly older ages of the cited poles (Fig. 6b, Table 2). Our pole is closest to the pole for the Eocene–Oligocene of the Ilpinsky Peninsula (Kovalenko, 1992), tectonically belonging to the Achaivayam–Valaginsky island arc (Shapiro, 1995; Levashova et al., 2000) or the South Koryak island arc segment (Kovalenko, 2003). Nevertheless, this pole is also statistically different from the one calculated in our study: $\gamma/\gamma_{cr} = 10.8°/10.1°$.

A nearly coeval pole calculated from the Oligocene–Miocene sediment layers of western Kamchatka (Kazansky et al., 2021) also differs significantly from the pole of the Pribrezhny complex: $\gamma/\gamma_{cr} = 22.9°/9.4°$, despite similar paleolatitude estimates of the corresponding blocks. This may indicate relative rotation of the blocks within Kamchatka after the formation of the volcanics of the Pribrezhny complex.

Thus, the paleomagnetic data show that the complexes of southern Kamchatka did not undergo significant latitudinal displacements after the formation of the volcanic rocks of the Pribrezhny complex, i.e., after the early Miocene. This is consistent with a model that favors the formation of the Pribrezhny complex on the continental crust of the Olyutor–Kamchatka folded system rather than within an independent "exotic" terrane (e.g., the Kronotsky block). The structural and geological data also support this idea. In the region of the Pribrezhny complex, mainly block deformations are observed, which resulted in the formation of a gently folded structure, in contrast to the nearby formations of the Kronotsky terrane in the region of Cape Shipunsky, which underwent more intense dislocations during the collision and are characterized by a more complex fold-and thrust structure (Tsukanov et al., 2022).

The presence of intrusive bodies with postfolding remanence (group 2 of normal polarity) somewhat contradicts the Early Miocene dating of the Pribrezhny complex, since the age of the main phase of deformations associated with the accretion of the Kronotsky terrane is estimated by most authors at 10–5 Myr (Levashova et al., 2000; Soloviev, 2008; Shapiro and Soloviev, 2009). This contradiction can be explained by the more ancient age of deformations in southern Kamchatka compared to the northern Kam-

chatka, or by our sampling of younger magmatic bodies in the Miocene Pribrezhny complex. For example, these bodies could be the normally magnetized basalt dikes in the Vilyuchinsk and the Zavoiko Peninsula regions, which cut through older magmatic rock massifs. These dikes are spatially confined to the Malka–Petropavlovsk zone of transverse faults and can be genetically related to the widespread Pleistocene–Holocene monogenic volcanism in this zone (Bergal-Kuvikas et al., 2022).

CONCLUSIONS

(1) Most of the sampled bodies of the Pribrezhny complex were formed before the main phase of tectonic deformations, probably associated with the accretion of the Kronotsky terrane. At the same time, part of the intrusive bodies contains postfolding remanent magnetization and may represent products of younger episodes of magmatism.

(2) The paleomagnetic pole for the Miocene of southern Kamchatka has been calculated from 33 sites of normal and reversed polarity. The calculated pole is statistically significantly different from all published Cenozoic poles in nearby regions.

(3) The paleomagnetic data indicate the formation of the volcanics of the Pribrezhny complex at a paleolatitude close to the present position (52.3°) and support the formation of the Miocene supra-subduction volcanic belt on the more ancient folded basement of the Olyutor–Kamchatka folded system rather than within a separate exotic block.

ACKNOWLEDGMENTS

We are grateful to T.E. Bagdasaryan and A.V. Chistyakova for helping in conducting electron microscopic studies and to D.V. Lastovetskii and A.N. Rogozin for helping in organizing field trips to the Pacific coast outcrops of southern Kamchatka. We also thank the reviewers for their valuable comments.

FUNDING

This work was supported by Russian Science Foundation under project no. 22-77-10019, https://rscf.ru/project/22-77-10019/.

CONFLICT OF INTEREST

The authors of this work declare that they have no conflicts of interest.

REFERENCES

Avdeiko, G.P., Palueva, A.A., and Khleborodova, O.A., Geodynamic conditions of volcanism and magma formation in the Kurile–Kamchatka island-arc system, *Petrology*, 2006, vol. 14, no. 3, pp. 230–246.

Bazhenov, M.L., Zharov, A.E., Levashova, N.M., Kodama, K., Bragin, N.Y., Fedorov, P.I., et al., Paleomagnetism of a Late Cretaceous island arc complex from South Sakhalin, East Asia: Convergent boundaries far away from the Asian continental margin?, *J. Geophys. Res.*, 2001, vol. 106, no. B9, pp. 19193–19205.

Bergal-Kuvikas, O., Bindeman, I., Chugaev, A., Larionova, Yu., Perepelov, A., and Khubaeva, O., Pleistocene-Holocene monogenetic volcanism at the Malko-Petropavlovsk zone of transverse dislocations on Kamchatka: Geochemical features and genesis, *Pure Appl. Geophys.*, 2022, vol. 179, no. 11, pp. 3989–4011.

Bergal-Kuvikas, O.V., Latyshev, A.V., Anosova, M.B., and Latanova, E.A., Expedition for the study Miocene igneous rocks to southern Kamchatka, *Vestn. KRAUNTs, Nauki Zemle*, 2022, no. 4, pp. 123–129.

Bogdanov, N.A. and Chekhovich, V.D., On the collision between the West Kamchatka and Sea of Okhotsk plates, *Geotectonics*, 2002, vol. 36, no. 1, pp. 63–75.

Day, R., Fuller, M., and Schmidt, V.A., Hysteresis properties of titanomagnetites: Grain size and composition dependence, *Phys. Earth Planet. Inter.*, 1977, vol. 13, pp. 260–267.

Debiche, M.G. and Watson, G.S., Confidence limits and bias correction for estimating angles between directions with applications to paleomagnetism, *J. Geophys. Res.*, 1995, vol. 100, no. B12, pp. 24405–24429.

Dunlop, D.J., Theory and application of the Day plot (*Mrs/Ms* versus *Hcr/Hc*) 1. Theoretical curves and tests using titanomagnetite data, *J. Geophys. Res.*, 2002, vol. 107, no. B3, Article ID 2056.

Enkin, R.J., *A Computer Program Package for Analysis and Presentation of Paleomagnetic Data*, Sidney, British Columbia: Pacific Geoscience Centre, Geological Survey of Canada, 1994.

Fisher, R., Dispersion on a sphere, *Proc. R. Soc. London, Ser. A: Math. Phys. Sci.*, 1953, vol. 217, no. 1130, pp. 295–305.

Gapeev, A.K. and Tsel'movich, V.A., *Stadii okisleniya titanomagnetitovykh zeren v izverzhennykh porodakh* (Oxidation Stages of Titanomagnetite Grains in Igneous Rocks), VINITI Deponent no. 1331-V89, Moscow: VINITI, 1989.

Haggerty, S.E., Oxidation of opaque mineral oxides in basalts, in *Oxide Minerals: Reviews in Mineralogy*, vol. 3, Rumble, D., Ed., Washington: Mineral. Soc. Am., 1976, pp. 1–98.

Kazansky, A.Yu., Vodovozov, V.Yu., Gladenkov, A.Yu., Gladenkov, Yu.B., and Trubikhin, V.M., Magnetostratigraphy of West Kamchatka marine Cenozoic key section (Kvachina Bay), *Stratigr. Geol. Correl.*, 2021, vol. 29, no. 1, pp. 104–119.

Khanchuk, A.I. and Grebennikov, A.V., The Late Miocene–Pliocene transform margin of Kamchatka, *Russ. J. Pac. Geol.*, 2021, vol. 15, no. 5, pp. 389–400.

Kirschvink, J.L., The leastsquare line and plane and the analysis of paleomagnetic data, *Geophys. J.R. Astron. Soc.*, 1980, vol. 62, pp. 699–718.

Konstantinov, K.M., Bazhenov, M.L., Fetisova, A.M., and Khutorskoy, M.D., Paleomagnetism of trap intrusions, East Siberia: Implications to flood basalt emplacement and the Permo-Triassic crisis of biosphere, *Earth Planet. Sci. Lett.*, 2014, vol. 394, pp 242–253. https://doi.org/10.1016/j.epsl.2014.03.029

Kovalenko, D.V., Paleomagnetism of the Paleogene complexes of the Ilpinsky Peninsula, *Geotektonika*, 1992, vol. 26, no. 5, pp. 78–95.

Kovalenko, D.V., *Paleomagnetizm geologicheskikh kompleksov Kamchatki i yuzhnoi Koryakii. Tektonicheskaya i geofizicheskaya interpretatsiya* (Paleomagnetism of the Geological Complexes in Kamchatka and Southern Koryak Highland. Tectonic and Geophysical Interpretation), Moscow: Nauchnyi mir, 2003.

Kovalenko, D.V. and Chernov, E.E., Paleomagnetism and tectonic evolution of Kamchatka and southern Koryakia, *Tikhookean. Geol.*, 2003, vol. 22, no. 3, pp. 48–73.

Lander, A.V. and Shapiro, M.N., The origin of the modern Kamchatka subduction zone, in *Volcanism and Subduction: The Kamchatka Region*, Eichelberger, J., Gordeev, E., Kasahara, M., Izbekov, P., and Lees, J., Eds., Geophys. Monogr. Ser., vol. 172, Washington: Am. Geophys. Union, 2007, pp. 57–64.

Latyshev, A.V., Veselovskiy, R.V., and Ivanov, A.V., Paleomagnetism of the Permian-Triassic intrusions from the Tunguska syncline and the Angara-Taseeva depression, Siberian Traps Large Igneous Province: Evidence of contrasting styles of magmatism, *Tectonophysics*, 2018, vol. 723, no. B11, pp. 41–55.
https://doi.org/10.1016/j.tecto.2017.11.035

Latyshev, A., Krivolutskaya, N., Ulyakhina, P., Fetisova, A., Veselovskiy, R., Pasenko, A., Khotylev, A., and Anosova, M., Paleomagnetism of the Permian-Triassic intrusions from the Norilsk region (the Siberian platform, Russia): Implications for the timing and correlation of magmatic events, and magmatic evolution, *J. Asian Earth Sci.*, 2021, vol. 217, no. 3, Article ID 104858.
https://doi.org/10.1016/j.jseaes.2021.104858

Latyshev, A., Radko, V., Veselovskiy, R., Fetisova, A., Krivolutskaya, N., and Fursova, S., Reconstruction of the magma transport patterns in the Permian-Triassic Siberian Traps from the northwestern Siberian Platform on the basis of anisotropy of magnetic susceptibility data, *Minerals*, 2023, vol. 13, no. 3, Article ID 446.
https://doi.org/10.3390/min13030446

Levashova, N.M., Shapiro, M.N., and Bazhenov, M.L., Late Cretaceous paleomagnetic data from the Median Range of Kamchatka, Russia: tectonic implications, *Earth Planet. Sci. Lett.*, 1998, vol. 163, nos. 1–4, pp. 235–246.

Levashova, N.M., Shapiro, M.N., Beniamovsky, V.N., and Bazhenov, M.L., Paleomagnetism and geochronology of the Late Cretaceous-Paleogene island arc complex of the Kronotsky Peninsula, Kamchatka, Russia: kinematic implications, *Tectonics*, 2000, vol. 19, no. 5, pp. 834–851.

Liu, Q., Deng, C., Yu, Y., Torrent, J., Jackson, M.J., Banerjee, S.K., and Zhu, R., Temperature dependence of magnetic susceptibility in an argon environment: Implications for pedogenesis of Chinese loess/palaeosols, *Geophys. J. Int.*, 2005, vol. 161, no. 1, pp. 102–112.
https://doi.org/10.1111/j.1365-246X.2005.02564.x

McEnroe, S.A., North America during the Lower Cretaceous: new palaeomagnetic constraints from intrusions in New England, *Geophys. J. Int.*, 1996, vol. 126, no. 2, pp. 477–494.

McFadden, P.L. and McElhinny, M.W., Classification of the reversal test in palaeomagnetism, *Geophys. J. Int.*, 1990, vol. 103, no. 3, p. 725–729.
https://doi.org/10.1111/j.1365-246X.1990.tb05683.x

Nikishin, A.M., Grevtsev, A.V., and Malyshev, N.A., History of formation of sedimentary basins of the seas of the Far East and Eastern Arctic, *Mater. XLII Tektonicheskogo soveshch. "Geologiya polyarnykh oblastei Zemli," tom 2* (Proc. XLII Tectonic Conf. "Geology of the Polar Regions of the Earth," vol. 2), Moscow: RAN, 2009, pp. 85–88.

Pechersky, D.M., Levashova, N.M., Shapiro, M.N., Bazhenov, M.L., and Sharonova, Z.V., Paleomagnetism of Palaeogene volcanic series of the Kamchatsky Mys Peninsula, east Kamchatka: the motion of an active island arc, *Tectonophyslcs*, 1997, vol. 273, pp. 219–237.

Shapiro, M.N., Late Cretaceous Achaivayam-Valagin volcanic arc (Kamchatka) and plate kinematics of the northern Pacifica, *Geotektonika*, 1995, vol. 29, no. 1, pp. 58–70.

Shapiro, M.N. and Soloviev, A.V., Formation of the Olyutorsky–Kamchatka foldbelt: a kinematic model, *Russ. Geol. Geophys.*, 2009, vol. 50, no. 8, pp. 668–681.

Sheimovich, V.S., *Gosudarstvennaya geologicheskaya karta Rossiiskoi Federatsii. Masshtab 1 : 200000. Seriya Yuzhno-Kamchatskaya. Listy: N-57-XXI (Severnye Koryaki), N-57-XXVII (Petropavlovsk-Kamchatskii), N-57-XXXIII (Mutnovskaya sopka). Ob"yasnitel'naya zapiska* (Scale 1 : 200000 State Geological Map of the Russian Federation. South Kamchatka Series. Sheets: N-57-XXI (Northern Koryaks), N-57-XXVII (Petropavlovsk-Kamchatsky), N-57-XXXIII (Mutnovskaya Sopka). Explanatory Note), St. Petersburg: VSEGEI, 2000.

Sheimovich, V.S. and Patoka, M.G., *Geologicheskoe stroenie zon aktivnogo kainozoiskogo vulkanizma* (Geological Structure of Zones of Active Cenozoic Volcanism), Moscow: Nedra, 1989.

Slyadnev, B.I., Khasanov, Sh.G., Krikun, N.F., et al., *Gosudarstvennaya geologicheskaya karta Rossiiskoi Federatsii. Masshtab 1 : 1000000 (tret'e pokolenie). Seriya Koryakskо-Kamchatskaya: List N-57—Petropavlovsk-Kamchatskii. Ob"yasnitel'naya zapiska* (Scale 1 : 1000000 State Geological Map of the Russian Federation (Third Generation). Koryak-Kamchatka Series: Sheet N-57—Petropavlovsk-Kamchatsky. Explanatory Note), St. Petersburg: VSEGEI, 2006.

Soloviev, A.V., *Izuchenie tektonicheskikh protsessov v oblastyakh konvergentsii litosfernykh plit metodami trekovogo datirovaniya i strukturnogo analiza, Trudy Geologicheskogo instituta RAN, vyp. 577* (Study of Tectonic Processes in Areas of Convergence of Lithospheric Plates by Methods of Track Dating and Structural Analysis, Transactions of the Geological Institute of RAS, vol. 577), Moscow: Nauka, 2008.

Soloviev, A.V., Shapiro, M.N., Garver, J.I., and Lander, A.V., Formation of the east Kamchatkan accretionary prism according to fission-track dating of zircons from terrigene rocks, *Russ. Geol. Geophys.*, 2004, vol. 45, no. 11, pp. 1237–1247.

Tsukanov, N.V., Luchitskaya, M.V., Portnyagin, M.V., Savelyev, D.P., Soloviev, A.V., and Hourigan, J.K., The gabbro–granodiorite magmatic complex of the Kronotsky paleoarc (Eastern Kamchatka): composition, age, and tectonic position, *Geotectonics*, 2022, vol. 56, no. 5, pp. 607–630.

Vaes, B., van Hinsbergen, D.J.J., and Boschman, L.M., Reconstruction of subduction and back-arc spreading in the NW Pacific and Aleutian Basin: Clues to causes of Cretaceous and Eocene plate reorganizations, *Tectonics*, 2019, vol. 38, no. 4, pp. 1367–1413.

Veselovskiy, R.V., Dubinya, N.V., Ponomarev, A.V., Fokin, I.V., Patonin, A.V., Pasenko, A.M., Fetisova, A.M., Matveev, M.A., Afinogenova, N.A., Rud'ko, D.V., and Chistyakova, A.V., Shared research facilities "Petrophysics, geomechanics and paleomagnetism" of the Schmidt Institute of Physics of the Earth RAS, *Geodyn. Tectonophys.*, 2022, vol. 13, no. 2, Article ID 0579.
https://doi.org/10.5800/GT-2022-13-2-0579

Watson, G. and Enkin, R., The fold test in paleomagnetism as a parameter estimation problem, *Geophys. Res. Lett.*, 1993, vol. 20, no. 19, pp. 2135–2137.
https://doi.org/10.1029/93gl01901

Zijderveld, J.D.A., AC demagnetization of rocks: Analysis of results, in *Methods in Palaeomagnetism*, Runcorn, S.K., Creer, K.M. and Collinson, D.W., Eds., Amsterdam: Elsevier, 1967, pp. 254–286.
https://doi.org/10.1016/j.neuroscience.2010.03.066

Zonenshain, L.P, Kuzmin, M.I., and Natapov, L.M., *Geology of the USSR: A Plate-Tectonic Synthesis*, Geodyn. Ser., vol. 21, Washington: AGU, 1990.

Translated by M. Nazarenko